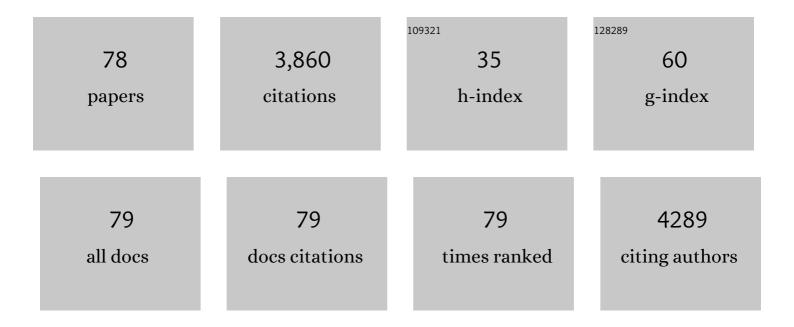
## **Richard N Collins**

List of Publications by Year in descending order

Source: https://exaly.com/author-pdf/1866646/publications.pdf Version: 2024-02-01



#	Article	IF	CITATIONS
1	The effect of silica and natural organic matter on the Fe(II)-catalysed transformation and reactivity of Fe(III) minerals. Geochimica Et Cosmochimica Acta, 2009, 73, 4409-4422.	3.9	318
2	Effect of Solution and Solid-Phase Conditions on the Fe(II)-Accelerated Transformation of Ferrihydrite to Lepidocrocite and Goethite. Environmental Science & Technology, 2014, 48, 5477-5485.	10.0	265
3	Advances in Surface Passivation of Nanoscale Zerovalent Iron: A Critical Review. Environmental Science & Technology, 2018, 52, 12010-12025.	10.0	225
4	Microbial communities reflect temporal changes in cyanobacterial composition in a shallow ephemeral freshwater lake. ISME Journal, 2016, 10, 1337-1351.	9.8	212
5	Speciation of metal(loid)s in environmental samples by X-ray absorption spectroscopy: A critical review. Analytica Chimica Acta, 2014, 822, 1-22.	5.4	150
6	Effect of Structural Transformation of Nanoparticulate Zero-Valent Iron on Generation of Reactive Oxygen Species. Environmental Science & amp; Technology, 2016, 50, 3820-3828.	10.0	124
7	Ferrous iron oxidation under acidic conditions – The effect of ferric oxide surfaces. Geochimica Et Cosmochimica Acta, 2014, 145, 1-12.	3.9	106
8	Chemical Forms of Selenium in the Metal-Resistant Bacterium Ralstonia metallidurans CH34 Exposed to Selenite andSelenate. Applied and Environmental Microbiology, 2005, 71, 2331-2337.	3.1	96
9	Effect of Amorphous Fe(III) Oxide Transformation on the Fe(II)-Mediated Reduction of U(VI). Environmental Science & Technology, 2011, 45, 1327-1333.	10.0	96
10	Effect of <i>Shewanella oneidensis</i> on the Kinetics of Fe(II)-Catalyzed Transformation of Ferrihydrite to Crystalline Iron Oxides. Environmental Science & Technology, 2018, 52, 114-123.	10.0	80
11	The aqueous phase speciation and chemistry of cobalt in terrestrial environments. Chemosphere, 2010, 79, 763-771.	8.2	79
12	Determination of Metalâ^'EDTA Complexes in Soil Solution and Plant Xylem by Ion Chromatography-Electrospray Mass Spectrometry. Environmental Science & Technology, 2001, 35, 2589-2593.	10.0	77
13	Labile Fe(III) from sorbed Fe(II) oxidation is the key intermediate in Fe(II)-catalyzed ferrihydrite transformation. Geochimica Et Cosmochimica Acta, 2020, 272, 105-120.	3.9	72
14	Characterisation of the Physical Composition and Microbial Community Structure of Biofilms within a Model Full-Scale Drinking Water Distribution System. PLoS ONE, 2015, 10, e0115824.	2.5	70
15	Anion exchange liquid chromatography–inductively coupled plasma-mass spectrometry detection of the Co2+, Cu2+, Fe3+ and Ni2+ complexes of mugineic and deoxymugineic acid. Journal of Chromatography A, 2006, 1129, 208-215.	3.7	69
16	Reduction of U(VI) by Fe(II) during the Fe(II)-Accelerated Transformation of Ferrihydrite. Environmental Science & Technology, 2014, 48, 9086-9093.	10.0	67
17	Redox characterization of the Fe(II)-catalyzed transformation of ferrihydrite to goethite. Geochimica Et Cosmochimica Acta, 2017, 218, 257-272.	3.9	63
18	Schwertmannite stability in acidified coastal environments. Geochimica Et Cosmochimica Acta, 2010, 74, 482-496.	3.9	61

#	Article	IF	CITATIONS
19	Influence of Dissolved Silicate on Rates of Fe(II) Oxidation. Environmental Science & Technology, 2016, 50, 11663-11671.	10.0	59
20	Uptake of intact zincâ€ethylenediaminetetraacetic acid from soil is dependent on plant species and complex concentration. Environmental Toxicology and Chemistry, 2002, 21, 1940-1945.	4.3	57
21	Water Recovery Rate in Short-Circuited Closed-Cycle Operation of Flow-Electrode Capacitive Deionization (FCDI). Environmental Science & amp; Technology, 2019, 53, 13859-13867.	10.0	57
22	Mineral species control of aluminum solubility in sulfate-rich acidic waters. Geochimica Et Cosmochimica Acta, 2011, 75, 965-977.	3.9	55
23	Flow-Electrode CDI Removes the Uncharged Ca–UO <sub>2</sub> –CO <sub>3</sub> Ternary Complex from Brackish Potable Groundwater: Complex Dissociation, Transport, and Sorption. Environmental Science & Technology, 2019, 53, 2739-2747.	10.0	54
24	Uranium Reduction by Fe(II) in the Presence of Montmorillonite and Nontronite. Environmental Science & Technology, 2016, 50, 8223-8230.	10.0	52
25	Phosphate recovery as vivianite using a flow-electrode capacitive desalination (FCDI) and fluidized bed crystallization (FBC) coupled system. Water Research, 2021, 194, 116939.	11.3	52
26	An in situ quick-EXAFS and redox potential study of the Fe(II)-catalysed transformation of ferrihydrite. Colloids and Surfaces A: Physicochemical and Engineering Aspects, 2013, 435, 2-8.	4.7	48
27	The short-term reduction of uranium by nanoscale zero-valent iron (nZVI): role of oxide shell, reduction mechanism and the formation of U( <scp>v</scp> )-carbonate phases. Environmental Science: Nano, 2017, 4, 1304-1313.	4.3	47
28	The tortoise versus the hare - Possible advantages of microparticulate zerovalent iron (mZVI) over nanoparticulate zerovalent iron (nZVI) in aerobic degradation of contaminants. Water Research, 2016, 105, 331-340.	11.3	46
29	Production of a Surface-Localized Oxidant during Oxygenation of Mackinawite (FeS). Environmental Science & Technology, 2020, 54, 1167-1176.	10.0	45
30	Arsenic (III) removal by mechanochemically sulfidated microscale zero valent iron under anoxic and oxic conditions. Water Research, 2021, 198, 117132.	11.3	45
31	Separation of low-molecular mass organic acid–metal complexes by high-performance liquid chromatography. Journal of Chromatography A, 2004, 1059, 1-12.	3.7	44
32	<i>Fodinomyces uranophilus</i> gen. nov. sp. nov. and <i>Coniochaeta fodinicola</i> sp. nov., two uranium mine-inhabiting Ascomycota fungi from northern Australia. Mycologia, 2014, 106, 1073-1089.	1.9	43
33	Reduced Uranium Phases Produced from Anaerobic Reaction with Nanoscale Zerovalent Iron. Environmental Science & Technology, 2016, 50, 2595-2601.	10.0	43
34	Enhanced anaerobic transformations of carbon tetrachloride by soil organic matter. Environmental Toxicology and Chemistry, 1999, 18, 2703-2710.	4.3	40
35	Use of fourier transform infrared spectroscopy to examine the Fe(II)-Catalyzed transformation of ferrihydrite. Talanta, 2017, 175, 30-37.	5.5	38
36	Key Considerations When Assessing Novel Fenton Catalysts: Iron Oxychloride (FeOCl) as a Case Study. Environmental Science & Technology, 2021, 55, 13317-13325.	10.0	37

#	Article	IF	CITATIONS
37	Organic Ligand and pH Effects on Isotopically Exchangeable Cadmium in Polluted Soils. Soil Science Society of America Journal, 2003, 67, 112.	2.2	37
38	Uranium Binding Mechanisms of the Acid-Tolerant Fungus <i>Coniochaeta fodinicola</i> . Environmental Science & Technology, 2015, 49, 8487-8496.	10.0	36
39	Dissociation kinetics of Fe(III)– and Al(III)–natural organic matter complexes at pH 6.0 and 8.0 and 25°C. Geochimica Et Cosmochimica Acta, 2009, 73, 2875-2887.	3.9	35
40	Applications of Time-Resolved Laser Fluorescence Spectroscopy to the Environmental Biogeochemistry of Actinides. Journal of Environmental Quality, 2011, 40, 731-741.	2.0	35
41	Effects of Good's Buffers and pH on the Structural Transformation of Zero Valent Iron and the Oxidative Degradation of Contaminants. Environmental Science & Technology, 2018, 52, 1393-1403.	10.0	35
42	Uptake, Localization, and Speciation of Cobalt in <i>Triticum aestivum</i> L. (Wheat) and <i>Lycopersicon esculentum</i> M. (Tomato). Environmental Science & Technology, 2010, 44, 2904-2910.	10.0	32
43	Pedogenic factors and measurements of the plant uptake of cobalt. Plant and Soil, 2011, 339, 499-512.	3.7	32
44	The reduction of 4-chloronitrobenzene by Fe(II)-Fe(III) oxide systems - correlations with reduction potential and inhibition by silicate. Journal of Hazardous Materials, 2016, 320, 143-149.	12.4	31
45	Assessment of Isotope Exchange Methodology to Determine the Sorption Coefficient and Isotopically Exchangeable Concentration of Selenium in Soils and Sediments. Environmental Science & Technology, 2006, 40, 7778-7783.	10.0	30
46	Resolving Early Stages of Homogeneous Iron(III) Oxyhydroxide Formation from Iron(III) Nitrate Solutions at pH 3 Using Time-Resolved SAXS. Langmuir, 2014, 30, 3548-3556.	3.5	29
47	An in situ XAS study of ferric iron hydrolysis and precipitation in the presence of perchlorate, nitrate, chloride and sulfate. Geochimica Et Cosmochimica Acta, 2016, 177, 150-169.	3.9	27
48	Reductive reactivity of borohydride- and dithionite-synthesized iron-based nanoparticles: A comparative study. Journal of Hazardous Materials, 2016, 303, 101-110.	12.4	26
49	Fe(II) Interactions with Smectites: Temporal Changes in Redox Reactivity and the Formation of Green Rust. Environmental Science & Technology, 2017, 51, 12573-12582.	10.0	26
50	Novel pattern of foliar metal distribution in a manganese hyperaccumulator. Functional Plant Biology, 2008, 35, 193.	2.1	23
51	Solid phases responsible for Mn II , Cr III , Co II , Ni, Cu II and Zn immobilization by a modified bauxite refinery residue (red mud) at pH 7.5. Chemical Engineering Journal, 2014, 236, 419-429.	12.7	22
52	Mechanisms and Rates of U(VI) Reduction by Fe(II) in Homogeneous Aqueous Solution and the Role of U(V) Disproportionation. Journal of Physical Chemistry A, 2017, 121, 6603-6613.	2.5	22
53	Fate of Plutonium at a Former Nuclear Testing Site in Australia. Environmental Science & Technology, 2016, 50, 9098-9104.	10.0	21
54	Speciation and transport of arsenic in an acid sulfate soil-dominated catchment, eastern Australia. Chemosphere, 2011, 82, 879-887.	8.2	19

#	Article	IF	CITATIONS
55	Donnan membrane speciation of Al, Fe, trace metals and REEs in coastal lowland acid sulfate soil-impacted drainage waters. Science of the Total Environment, 2016, 547, 104-113.	8.0	19
56	Iron Transformation and Its Role in Phosphorus Immobilization in a UCT-MBR with Vivianite Formation Enhancement. Environmental Science & Technology, 2020, 54, 12539-12549.	10.0	19
5 <b>7</b>	Resistance, accumulation and transformation of selenium by the cyanobacterium Synechocystis sp. PCC 6803 after exposure to inorganic SeVI or SeIV. Radiochimica Acta, 2005, 93, 683-689.	1.2	17
58	Exchangeable and secondary mineral reactive pools of aluminium in coastal lowland acid sulfate soils. Science of the Total Environment, 2014, 485-486, 232-240.	8.0	17
59	Impact of reactive iron in coal mine dust on oxidant generation and epithelial lung cell viability. Science of the Total Environment, 2022, 810, 152277.	8.0	15
60	Inhibition of Uranium(VI) Sorption on Titanium Dioxide by Surface Iron(III) Species in Ferric Oxide/Titanium Dioxide Systems. Environmental Science & Technology, 2012, 46, 11128-11134.	10.0	14
61	Metal(loid) Bioaccessibility Dictates Microbial Community Composition in Acid Sulfate Soil Horizons and Sulfidic Drain Sediments. Environmental Science & Technology, 2014, 48, 8514-8521.	10.0	14
62	Influence of thermodynamic database on the modelisation of americium(III) speciation in a simulated biological medium. Radiochimica Acta, 2005, 93, 715-718.	1.2	12
63	Potential phytoavailability of anthropogenic cobalt in soils as measured by isotope dilution techniques. Science of the Total Environment, 2008, 406, 108-115.	8.0	12
64	Uranium extraction from a low-grade, stockpiled, non-sulfidic ore: Impact of added iron and the native microbial consortia. Hydrometallurgy, 2017, 167, 81-91.	4.3	12
65	Immobilisation of geogenic arsenic and vanadium in iron-rich sediments and iron stone deposits. Science of the Total Environment, 2019, 654, 1072-1081.	8.0	12
66	The impacts of low-cost treatment options upon scale formation potential in remote communities reliant on hard groundwaters. A case study: Northern Territory, Australia. Science of the Total Environment, 2012, 416, 22-31.	8.0	11
67	Soil- and surfactant-enhanced reductive dechlorination of carbon tetrachloride in the presence of Shewanella putrefaciens 200. Journal of Contaminant Hydrology, 1997, 28, 337-361.	3.3	10
68	Transformation and fixation of Zn in two polluted soils by changes of pH and organic ligands. Soil Research, 2003, 41, 905.	1.1	10
69	Anodic Reactivity of Ferrous Sulfide Precipitates Changing over Time due to Particulate Speciation. Environmental Science & Technology, 2013, 47, 12366-12373.	10.0	9
70	Isotopically Exchangeable Concentrations of Elements Having Multiple Oxidation States: The Case of Fe(II)/Fe(III) Isotope Self-Exchange in Coastal Lowland Acid Sulfate Soils. Environmental Science & Technology, 2009, 43, 5365-5370.	10.0	8
71	Investigating the effect of ascorbate on the Fe(II)-catalyzed transformation of the poorly crystalline iron mineral ferrihydrite. Biochimica Et Biophysica Acta - General Subjects, 2018, 1862, 1760-1769.	2.4	8
72	Influence of calcium and silica on hydraulic properties of sodium montmorillonite assemblages under alkaline conditions. Journal of Colloid and Interface Science, 2010, 343, 366-373.	9.4	7

#	Article	IF	CITATIONS
73	Radioactive particles from a range of past nuclear events: Challenges posed by highly varied structure and composition. Science of the Total Environment, 2022, 842, 156755.	8.0	5
74	Seleno-l-Methionine Is the Predominant Organic Form of Selenium in Cupriavidus metallidurans CH34 Exposed to Selenite or Selenate. Applied and Environmental Microbiology, 2006, 72, 6414-6416.	3.1	4
75	Impact of soil consolidation and solution composition on the hydraulic properties of coastal acid sulfate soils. Soil Research, 2008, 46, 112.	1.1	4
76	Improved detection of coastal acid sulfate soil hotspots through biomonitoring of metal(loid) accumulation in water lilies (Nymphaea capensis). Science of the Total Environment, 2014, 487, 500-505.	8.0	4
77	Assessment of uranium and selenium speciation in human and bacterial biological models to probe changes in their structural environment. Radiochimica Acta, 2009, 97, 375-383.	1.2	3
78	Isotopically exchangeable Al in coastal lowland acid sulfate soils. Science of the Total Environment, 2016, 542, 129-135.	8.0	1